ISSN 2304-3415, Russian Open Medical Journal
2024. Volume 13. Issue 1 (March). Article CID e0104
DOI: 10.15275/rusomj.2024.0104

Original article

A microchip for exosome isolation that can be impregnated with imatinib simultaneously: an in vitro analysis

Amir Monfaredan [1], Fakher Rahim [2], Gholamreza Tavoosidana [1], Mohammad Hossein Modarressi [1], Alaviyehsadat Hosseininasab [3], Ali-Akbar Aghajani-Afrouzi [4], Mahdi Shafiee Sabet [1], Elahe Motevaseli [1]

[1] Tehran University of Medical Sciences, Tehran, Iran
[2] Cihan university-Sulaymaniya, Kurdistan region, Iraq
[3] GeneDia Life science company, Tehran, Iran
[4] Payame Noor University, Tehran, Iran

Received 20 January 2024, Revised 8 February 2024, Accepted 12 February 2024

© 2024, Russian Open Medical Journal

Abstract: *Background and Aims* — Exosomes, which are tiny double-layered membranes originating from eukaryotic cells, have been recognized as a valuable natural vehicle for delivering substances because of their optimal size, compatibility with living organisms, strong structure, ability to carry a large amount of cargo, and capacity to be modified on their surface.
Methods — Various strategies have been employed to isolate exosomes due to the challenges associated with maintaining their high purity. The current investigation utilized a soft lithography technique to fabricate channels for exosome separation, incorporating immunoaffinity capabilities. Both biochemical and biophysical assays were conducted to assess the quality of isolated exosomes from various sources (serum, cell supernatant, and urine) and compared with a commercially available kit.
Results — The current investigation employed a microfluidic method to capture CD63-conjugated magnetic beads, resulting in a very effective separation of exosomes. Based on the data, there were no notable variations in miRNAs that were statistically significant. This demonstrates that the engineered chip successfully achieved the separation of the exosome while preserving the integrity of its nucleic acid components.
Conclusion — The results shown that the current methodology effectively isolated exosomes with a high yield rate, purity, and minimal time requirement. The imatinib laden exosomes demonstrated anticancer efficacy against the KYO-1 cell line in all of their forms.

Keywords: personalized medicine, exosome, laboratory on a chip, leukemia, targeted therapy.

Cite as Monfaredan A, Rahim F, Tavoosidana G, Modarressi MH, Hosseininasab A, Aghajani-Afrouzi AA, Sabet MS, Motevaseli E. A microchip for exosome isolation that can be impregnated with imatinib simultaneously: an in vitro analysis. *Russian Open Medical Journal* 2024; 13: e0104.

Correspondence to Elahe Motevaseli. E-mail: e_motevaseli@tums.ac.ir.

Introduction

Extracellular vehicles (EVs), also known as exosomes, have emerged as a prominent area of study due to their significant involvement in both biological processes and their potential as biocompatible carriers for diagnostics and therapy [1]. The utilization of exosomes in biomedical diagnosis and therapy has emphasized the pressing want for novel technologies in expeditious and precise techniques of exosome isolation in bodily fluids. Exosomes, which contain biomolecules such as proteins and nucleic acids (including mRNAs, microRNAs, and DNA), have been extensively studied for their diagnostic and therapeutic capabilities. This is due to their involvement in cell-to-cell communication and their potential for drug administration. A significant problem lies in addressing the intricate nature of fluid systems and the absence of effective methods for separation [2-4]. Exosomes are extracellular vesicles that contain lipids, proteins, and nucleic acids that are generated from cells. They can be detected in a variety of bodily fluids and contribute to both normal and abnormal physiological processes. A significant obstacle in the advancement of exosome research lies in the challenge of efficiently isolating pure exosomes from unwanted substances present in bodily fluids, despite their promising potential for use in medical diagnosis and treatment. So far, several methods have been suggested and studied for the separation of exosomes. Among these methods, microfluidic technology is the most promising option since it is relatively simple, cost-effective, and capable of precise and quick processing and automation at a small scale. Specifically, the elimination of exosome labelling is a notable improvement in terms of streamlining the procedure, reducing time and expense, and maintaining the biological functions of exosomes. Although there have been significant advancements in microfluidic techniques for isolating exosomes and the label-free methods have several benefits for clinical applications, current microfluidic platforms for exosome isolation still encounter various problems and obstacles that impede their effectiveness in sample processing [5-8]. Recent advances in microfluidic platforms for label-free exosome isolation are the subject of this study. These platforms incorporate various forces such as viscoelastic, acoustic, inertial, electrical, and centrifugal forces, and are based on various

concepts such as sieving, deterministic lateral displacement, field flow, and compressive flow fractionation [9-11].

Microfluidics has facilitated the development of novel techniques for purifying exosomes in recent years. Microfluidics offers systems, such as channels with dimensions in the micrometer range, for manipulating small volumes of fluids, ranging from microliters to picoliters. Most microfluidic devices are built using a specific polymer called poly dimethyl siloxane) or PDMS [3, 12, 13]. PDMS possesses optical transparency and biocompatibility, rendering it a valuable substance for fabricating biofluidic devices. Microfluidic platforms enable the accurate categorization of exosomes with a notable level of purity and sensitivity, while simultaneously decreasing the expenses, duration, and quantity of necessary substances. The immunoaffinity-based microfluidic technology for exosome isolation addresses the limitations of previous methods (such as ultracentrifugation, density gradient centrifugation, tangential flow filtering, and size-exclusion chromatography) by offering adjustability, automation, scalability, and portability. Exosomes can be separated from other constituents of the sample by utilizing specific proteins with identical characteristics. CD9, CD41, CD63, and CD81, along with molecules like as heparin, Tim4, and heat shock protein-binding peptides, are frequently used as surface markers for immunoaffinity-based extraction of exosomes [14-17].

In this study, we have created microfluidic devices to separate exosomes from various sources by utilizing magnetic beads that are coupled with CD68 [4, 18, 19].

Material and Methods

COMSOL simulations

Using the Multiphysics software COMSOL version 5.1, the channel governing equations were computed. Given its thinness, the flow was modelled as a single-phase laminar flow using the physical parameters of distilled water at ambient temperature and pH = 7.4. The following set of parameters were optimized: chip height, number of mazes, channel width at input and output, input flow rate, angle of position along chip length, radius of curvature of the curved channel, and channel width at design.

Chip construction

A microchip for isolating exosomes and loading it with imatinib was manufactured using a conventional soft lithography process. A layer of SU8 photoresist was applied to the silicon wafer from Microchem. Corp. in Newton, MA. A 4-inch wafer was coated with 5 cc of SU8 photoresist using spin coating at 2300 rpm. Following the spin coat, the wafers were baked at 60 degrees Celsius for 2 hours and 95 degrees Celsius for 15 minutes. Once the baking was finished, the UV lamp was turned on at 360 mV for 12 minutes on the SU8-coated wafer, and the mask was carefully positioned. Once the exposure was complete, the channels were observed after 4 minutes of washing with developer and 8 minutes of washing with isopropanol, respectively. Bubbles were created by mixing Polydimethylsiloxane (PDMS) (Microchem. Corp., Newton, MA) with hardener at a 1:10 ratio after the mold had been made. The PDMS chip was created by pouring 10 cc of PDMS and hardener solution over the mold and then leaving it to incubate at room temperature for 24 hours. Attaching the PDMS chip to the glass followed stimulation of the gel with plasma gas at a power of 12 mJ/min for 4 minutes after the gel had fully formed (*Supplementary, Figure S1*).

AFM microscopy

Under AFM microscopy, the monolayer thickness, surface roughness, magnetic properties, phase image, and friction image are examined. After being washed with acetone and dried at 60 °C, the chip was examined for changes in level as well as post and channel heights.

Microfluidic-based exosome extraction

For this portion of the investigation, the main sources of exosomes were serum, urine, and cell culture supernatant. The Anti-CD63 antibody from Abcam in the UK was linked to Mag nanoparticles obtained from Jiayuan Quantum Pickup Company in Wuhan, China using standard techniques. The nanoparticles have a binding capacity of approximately 10 µg of CD63 antibody per 1 mg of nanoparticles when employing a concentration of 1 mg/mL of Mag-CD63. The exosome-containing sample was combined with CD63-Mag and introduced into the microfluidic device through input 1. The anti-CD63 (Abcam, UK) was subsequently reintroduced through input 2. The Mag-CD63-Exo complex was formed by mixing flows from a twin syringe pump with a flow rate of 1-10 µL/min in the first channel. The immunomagnetic particles, namely CD63-Mag, were captured and held in chamber 1 using a magnetic disc. The Exo-CD63-Mag complex was washed by introducing the PBS buffer from input 3. Subsequently, it was stored in compartment 2. Exosomes that were conjugated with an immune component were gathered for analysis. The exosomes obtained from serum, urine, and cellular supernatant are extracted using specialized chips called S-EXOChip, UE-EXOChip, and SU-EXOChip, respectively. Additionally, the 4-gate input is specifically designated for drug loading and will be further explored (*Supplementary, Figure S2*).

Exosomes protein content

The protein content of the exosomes was determined using the Bradford method. Bovine serum albumin (BSA, Sigma, CAS no., 9048-46-8) at concentrations of 0.10, 0.08, 0.06, 0.04, and 0.02 mg/mL was employed, and the absorbance was measured at 595 nm [20].

Flow cytometry analysis

The accuracy of the exosome extraction was assessed by conducting flow cytometric analysis using an anti-CD63 antibody (Padza Padtenpajooh, cat#MM108, Iran) on the extracted samples, following the manufacturer's instructions. Concisely, 5 mg per test was introduced into the tubes containing exosomes, followed by gentle mixing and incubation in the absence of light for 60 minutes at a temperature range of 2-8 ° C. Subsequently, we cleansed the samples by employing 1 mL of diluted assay buffer 1X. In order to gather the magnetic grains, microtubes were positioned within a magnetic circuit and thereafter subjected to centrifugation at a speed of 3500×rpm for a duration of 10 minutes. An additional 350 µL of assay buffer 1X is introduced into the tube and subjected to analysis using a flow cytometer (Millipore Merck Germany).

© 2024, LLC Science and Innovations, Saratov, Russia

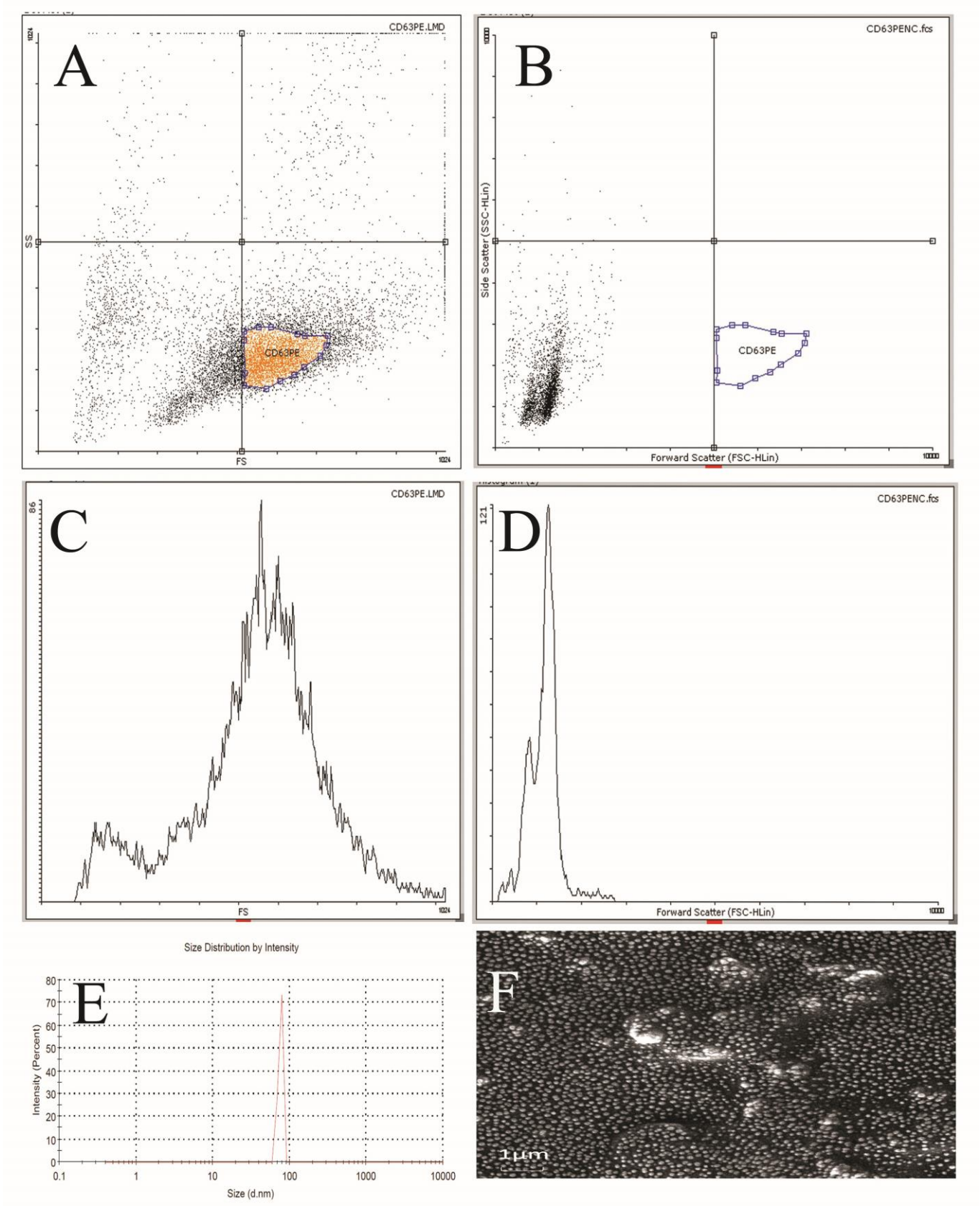

Figure 1. (A) The Flow cytometry analysis of the sample extracted by the chip against the CD68-PE antibody. (B) The chip extracted the sample in the presence of protease enzymes. (C) Chip-extracted sample histogram (D) Chip-extracted sample histogram in presents of protease enzymes. (E) The DLS histogram of isolates exosomes. (F) The SEM images of extracted exosomes.

© 2024, LLC Science and Innovations, Saratov, Russia

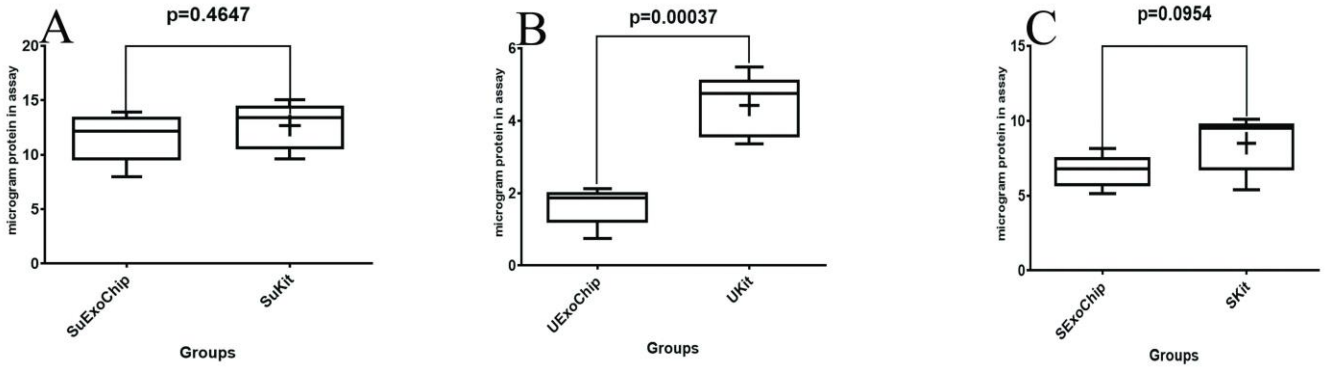

Figure 2. The protein content of the (A) cell supernatant, (B) urinary exosomes, and (C) serum using SU-8 100 chip commercially available kit with Bradford.

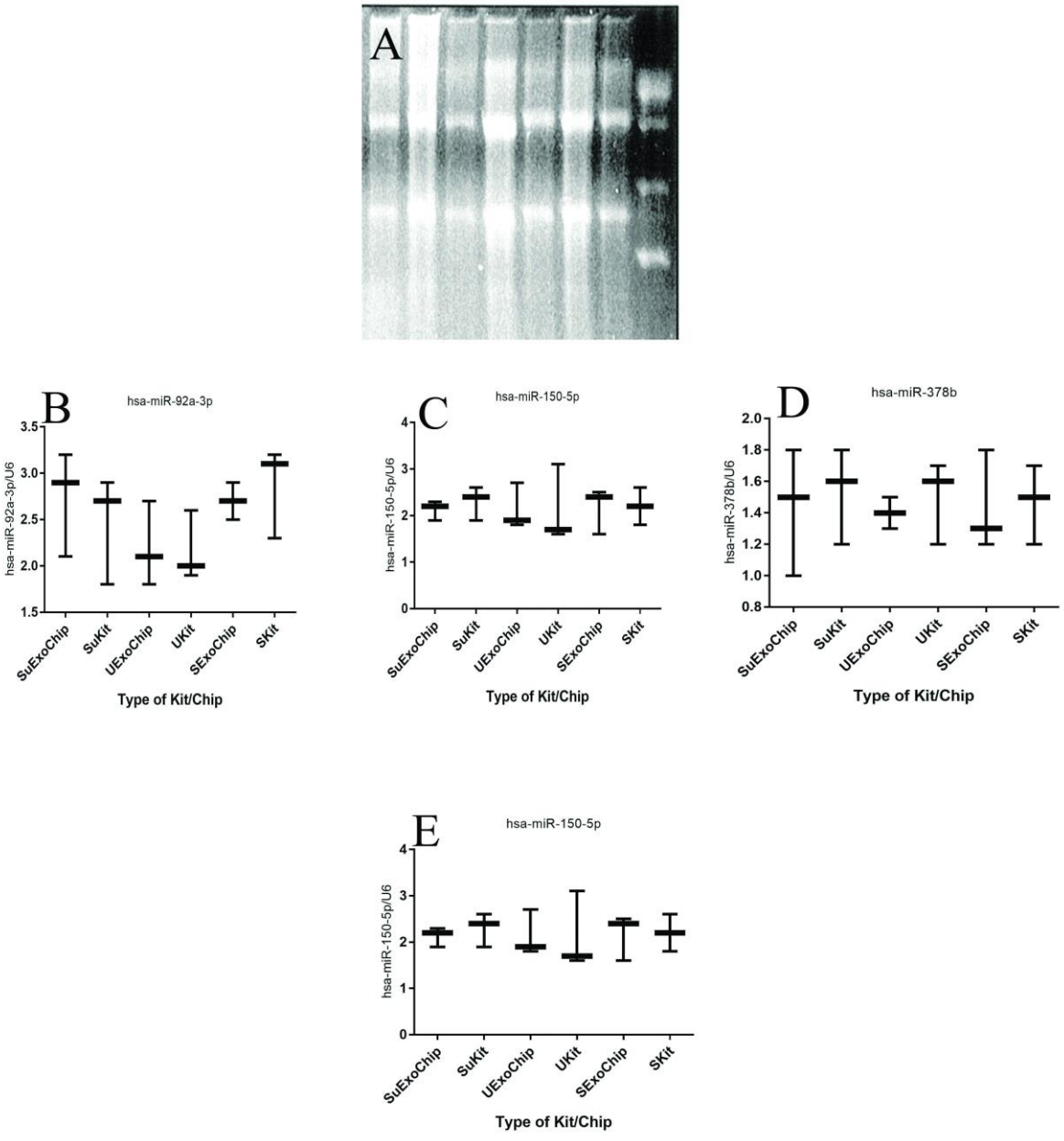

Figure 3. (A)The RNA extraction quality of exosome samples of serum, urine and cell supernatant using 2% agarose gel electrophoresis. The relative expression of (B) miR-92a-3p, (C) miR-150-5p, (D) miR-378, and (E) miR-155-5p in exosome samples of serum, urine, and cell supernatant using SU-8 100 chip and commercially available kit. The significance changes related to the RNA content of the experiment were analyzed using an unpaired t-test with a threshold of P<0.05.

© 2024, LLC Science and Innovations, Saratov, Russia

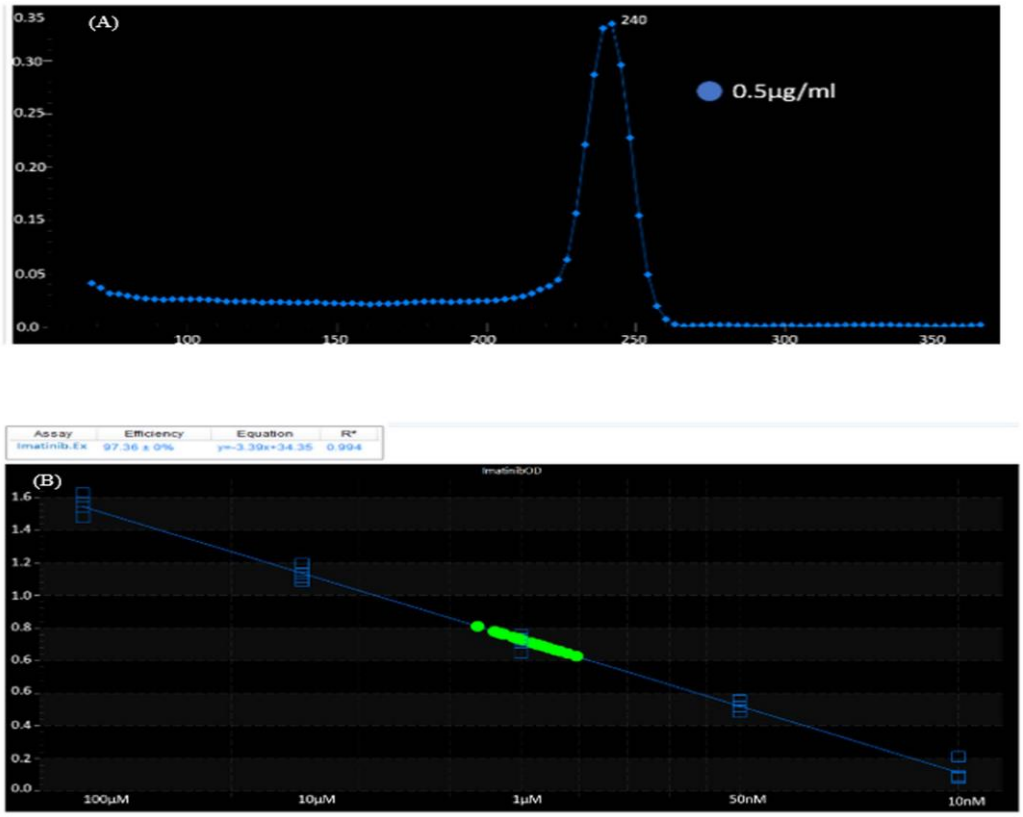

Figure 4. (A) The UV-Visible spectra of the imatinib-loaded CD63-Mag captured exosome with chip. (B) The linear equation of imatinib in PBS solution.

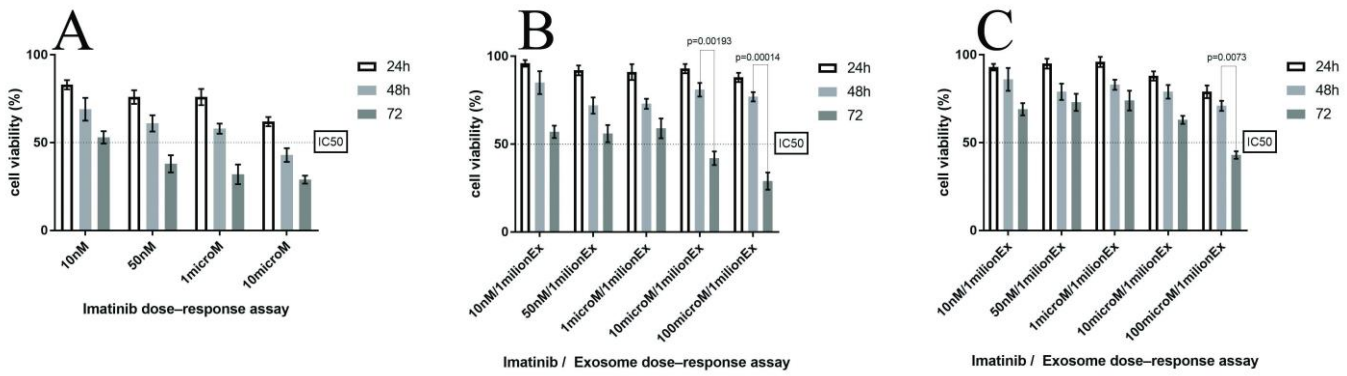

Figure 5. Cell viability at 24, 48 and 72h of incubation by treating cells with (A) free imatinib, (B) imatinib-loaded CD63-Mag captured exosome with the chip, and (C) imatinib-loaded exosome using the commercially available kit.

Exosome size and morphology analysis

To determine the hydrodynamic size using DLS analysis, 200 µL of the exosomal solution obtained from the cell supernatant was mixed with 420 µL of filtered PBS to create a diluted solution. Subsequently, the specimen was placed on ice and subjected to sonication for a duration of 10 minutes. Subsequently, the sample was introduced into a Dynamic Light Scattering (DLS) apparatus, where it was exposed to a laser light beam with a wavelength of 632 nm. The obtained data were then processed and evaluated using the Zeta Sizer software. The exosomes were analyzed for their size and shape using scanning electron microscopy (SEM). The exosomes were coated using an FEI Nova 200 Nanolab Dual-beam FIB scanning electron microscope at low energy levels (2.0-5.0 kV) in the Electron Microscopy Analysis Laboratory (MC2). This was done using gold spraying or carbon thermal evaporation. Subsequently, a volume of 200 µL of exosomes obtained from the cell supernatant was applied onto the slide and allowed to air-dry for one hour at ambient temperature. Subsequently, the sample was examined using electron microscopy.

Western blotting

Both extracted samples were supplemented with 50 µL of lysis buffer, containing a 1% concentration of Holt protease inhibitor (Thermofisher scientific, LTD, USA), and incubated at room temperature for 2 minutes. Subsequently, the samples were cooled on ice for a duration of 10 minutes and subjected to centrifugation at a speed of 13000× rpm for a period of 15 minutes at a temperature of 4°C. Ultimately, the samples were preserved

© 2024, LLC Science and Innovations, Saratov, Russia

at a temperature of -80°C in order to facilitate subsequent analysis. Analyzed in this study was the total volume of 20 µL for each sample using a 12% SDS polyacrylamide gel (SDS-PAGE). This gel is employed to separate proteins and ascertain their molecular weights, with a voltage intensity of 80 mV. CD81, a surface membrane-specific exosome protein, was identified in the cell lysate after separating the protein bands of the material using SDS-PAGE gel. To assemble an immunoblot cassette and load the gel and nitrocellulose paper onto the blotting apparatus (Biorad, USA). The protein bands were transferred for a duration of 90 minutes at a voltage of 100 millivolts. Subsequently, the membrane was rinsed in the blocking buffer for 60 minutes at a temperature of 37°C. Subsequently, the samples were treated with Anti-CD81 antibodies (diluted at a ratio of 1:4000) in TBS buffer (at a concentration of 1x). The antibody solution was then applied onto a PVDF membrane and the membrane was incubated in a shaker at a temperature of 37 °C for a duration of 37 hours. Subsequently, the specimen underwent three cycles of washing using TBS buffer, with each cycle lasting 10 minutes.

Exosomal extraction of RNA and measurement of miRNA expression levels

The process of extracting RNA was carried out using Norgen's Exosome RNA Isolation Kit (Cat# 58000) following the instructions provided by the manufacturer. At first, 300 µL of lysis buffer A and 37.5 µL of lysis buffer additive were added to each isolated exosome sample. Then, the samples were well mixed by vortexing for 10 seconds. Following a 10-minute incubation at room temperature, 500 µL of 96% ethanol was introduced to the mixture and thoroughly blended with Vertex for a duration of 10 seconds. Subsequently, 500 µL of the mixture was transferred to the Mini Spin column and subjected to centrifugation at a speed of 6000×rpm for a duration of 1 minute. After performing the previous step again, 600 µL of washing solution A was introduced into the column and subjected to centrifugation at a speed of 13000×rpm for 30 seconds, followed by an additional centrifugation at the same speed for 1 minute. Subsequently, a 50 µl aliquot of wash solution A was introduced onto the column and subjected to centrifugation at a speed of 8000×rpm for a duration of 1 minute. The resulting mixture is then stored at a temperature of -80 °C for subsequent analysis.

The cDNA extraction kit (ABM excellent Cat# G902) was used to convert the total non-coding RNAs and short RNAs, including miRNAs, into cDNA. The miRNA sample was generated by combining 2 µL of 5X poly (A) polymerase reaction buffer, 1.5 µL of ATP (10 mM), µL of MnCl2 (25 mM), 0.5 µL of Poly (A) Polymerase, Yeast (1 µg/µL), and 2.5 µL of H2O. Subsequently, the concoction was subjected to incubation for a duration of 30 minutes at a temperature of 37 degrees Celsius. Subsequently, the remaining material was supplemented with 2 µl of miRNA Oligo (dT) adaptor at a concentration of 10 mM. The solution was subjected to incubation at a temperature of 65 °C for a duration of 5 minutes, and subsequently cooled on a bed of crushed ice. Subsequently, 1 microliter of deoxyribonucleotide triphosphates (dNTPs) with a concentration of 10 millimolar, 4 microliters of 5-fold diluted reverse transcription (RT) buffer, 1 microliter of reverse transcriptase (RTase) with an activity of 200 units per microliter, and 2 microliters of water were introduced into the aforementioned combination. The cDNA synthesis was conducted by subjecting the materials to incubation at 42 °C for 15 minutes, followed by incubation at 70 °C for 10 minutes. The miRCURY™ LNATM microRNA Array Hy3™/Hy5™ kit (Exiqon, Denmark) was used to evaluate the microRNA concentration of materials from three sources: urine, serum, and cellular supernatant. The analysis followed the normal protocols. Exosome isolation was performed using the Norgen Exosome Isolation Kit (Cat#58000) on samples obtained from three different sources: urine, serum, and cellular supernatant. The qRT-PCR analysis was conducted for each sample using three Real-time PCR Systems, adhering to the manufacturer's instructions and employing distinct primers (Table I). A solution was generated by combining 7 µL of Exiqon PCR Mastermix, 0.5 µL of panel Primer (5 pmol/µL), 3 µL of Tailed cDNA, 3 µL of Enhancer, and 4 µL of DEPC Treated water. The procedure involved assessing the relative expression of miRNA-155 using U6 as a housekeeping control.

Drug loading

The revised approach involves directly incubating the medicines and CD63-Mag collected exosomes, followed by a freeze-thaw cycle, to enhance the loading of imatinib. The exosomes were subjected to incubation with imatinib at various doses. A volume of 10 nanomolar (nM) imatinib was injected into input 4 of the chips at a flow rate of 1 microliter per minute. The injection was performed at a temperature of 25 degrees Celsius for a duration of 20 minutes. Subsequently, papain and trypsin, both with concentrations of 0.1% and 0.02% respectively, were injected into the channel at a flow rate of 1 µL/min.

Drug release

The release of imatinib was investigated using a dialysis bag. 3 micrograms of exosome were homogenized in 3 milliliters of PBS buffer. The resulting mixture was then transferred to a dialysis bag and placed in a sealed container containing 60 milliliters of PBS buffer with a pH of 7.4. The temperature was maintained at a stable 37 degrees Celsius. The discharged imatinib content was determined by calculating the absorbance at a wavelength of 242 nm using UV-Visible spectroscopy. The standard curve was constructed using concentrations of 1, 2, 5, 10, 15, 20, and 25.30 µg/mL in a PBS solution.

Cell toxicity

The MTT assay was employed to assess the cytotoxicity of imatinib-loaded CD63-Mag collected exosomes against the KYO-1 cell line. The cellular metabolism of the cells was assessed by monitoring the activity of mitochondrial dehydrogenase enzymes using methyl thiazole tetrazolium bromide (MTT) as a substrate. For this purpose, a total of 10,000 cells were pre-cultured in 96 well plates and incubated for 24 hours at a temperature of 37 °C with a CO2 concentration of 4% and humidity level of 90%. The exosomal samples were treated with several doses ranging from 2 to 100 mg/ml for durations of 24, 48, and 72 hours. Subsequently, 20 µL of MTT solution with a concentration of 10 mg/mL was added to each well and incubated for 4 hours under the same conditions as mentioned earlier. Afterwards, the liquid portion above the sediment was removed and 100 µL of DMSO was introduced into each well. The mixture was agitated for 8 minutes in a circular pattern, and subsequently, the amount of formazan absorbed at a wavelength of 490 nm was determined using an

© 2024, LLC Science and Innovations, Saratov, Russia

ELISA reader. The cell viability percentage (IC50) was assessed using Graphpad Prism 6.0 software from the United States.

Statistical analysis

The statistical data were analyzed using Prism 7.0 software developed by GraphPad Software in the United States. The significance of RNA amounts and the validity of miRNAs among exosomes were assessed using a single direct T-test. A p-value less than 0.05 was deemed to have statistical significance.

Results

The current investigation employed a microfluidic method to capture CD63-conjugated magnetic beads, resulting in a very effective separation of exosomes. The PDMS chip mold is constructed from a silicon wafer patterned with SU-8 100 using the conventional soft lithography process. This mold possessed an immunoaffinity function, as depicted in *Figures* S3. The AFM images provided a visual representation of the chip's surface. The SU-8 100 surface is depicted in both two-dimensional (2D) and three-dimensional (3D) views (*Figure* S4). The exosomes were isolated using CD68-Mag, and their physicochemical characteristics were examined by several techniques including DLS (Dynamic Light Scattering), SEM (Scanning Electron Microscopy), flow cytometry, Bradford assay, qRT-PCR (quantitative Reverse Transcription Polymerase Chain Reaction), and western blotting analysis. Exosome samples were analyzed using flow cytometry in the presence and absence of a protease enzyme (*Figure* 1A-D). The hydrodynamic dimensions of the exosomes isolated from different biological sources were assessed using both a commercially available kit and an SU-8 100 chip. The hydrodynamic size distribution of isolated exosomes was depicted in Figure 1E using DLS analysis. The analysis estimated that the majority of exosomes had a mean diameter of 135 nm. *Figure* 1F displays the image obtained from the SEM examination. Visible evidence indicates the presence of exosomes that possess a spherical morphology, with a size ranging from 30 to 175 nm in diameter. *Figure* 2 presents a comparative analysis of protein contents in cell supernatant and urine generated exosomes utilizing chip and kit methods, together with the semi-quantitative Bradford approach. Both approaches did not cause substantial changes in the protein composition of serum and cellular supernatant. Regarding urinary extracted exosomes, while the commercially available protein content exhibited a notable increase, the proteins derived from the exosomes retrieved using the chip demonstrated more uniformity.

Investigation of the expression profile of exosome microRNAs

Following the extraction of RNA under conditions free of RNase, agarose gel electrophoresis was conducted to verify the integrity and quality of the RNAs. The absence of RNA degradation could be determined in gel testing by the presence of ribosomal S28, S18, and S5 bands. Furthermore, the presence of mRNA was indicated by the smear found between these two bands (*Figure* 3A). The diagram illustrates the y-axis representing microRNA expression, specifically in relation to its reference gene, U6. The horizontal axis displays the source of the exosome samples, which were obtained using a commercially available kit and chip developed for this research. Based on the data presented in *Figures* 3B to 3E and Table II, there were no notable variations in miRNAs that were statistically significant. This demonstrates that the engineered chip successfully achieved the separation of the exosome while preserving the integrity of its nucleic acid components.

The imatinib release

The study aimed to examine the efficacy of preserving the drug carrier structure, specifically the exosome, in facilitating drug release. To investigate this, the release of imatinib from retrieved exosomes was analyzed by utilizing both imatinib-loaded CD63-Mag collected exosomes using a chip. *Figure* 3A displayed the adsorption peak obtained from the imatinib solution in PBS. The absorption peak of imatinib was observed at a wavelength of 242±1 nm. A calibration curve with an R2 value of 0.994 was produced to assess the rate at which the medication is released (*Figure* 4).

Cell toxicity assessments

A comparative study was conducted to assess the impact of free imatinib, imatinib-loaded CD63-Mag caught exosome with chip, and a commercially available kit on the survival rate of the KYO-1 cell line. *Figures* 5A to 5C demonstrate that the toxicity of free imatinib, imatinib-loaded CD63-Mag caught exosome with chip, and available kits on KYO-1 cells is depending on the dosage. Furthermore, upon treating the cells with the extracted exosome using a commercially available kit, the dosage required for effectiveness was adjusted to 100 µmol. It is important to highlight that this adjustment was made possible by the chip's ability to preserve the structure and morphology of the retrieved exosome over time. The effective dose was comparable to the direct treatment of cells with imatinib.

Discussion

The potential of exosomes as a fluid biopsy for the identification of cancer biomarkers has garnered increasing attention during the past decade. Research like these has shown how critical it is to develop innovative methods for accurately and quickly separating exosomes from bodily fluids with little sample preparation time required [21-25]. Serious problems with purity and more intact performance arise when exosomes are exposed to contaminants and mechanical damage. Isolation, molecular analysis, and detection are just a few areas where the microfluidic-based exosome extraction approaches outperform their predecessors. Detection limits of around 50 exosomes/µL were achieved with the use of microfluidic technology, allowing for high-capacity exosome analyses of up to 100 µL/min [3, 26, 27].

Recent advances in the study of exosomes have shown their intimate relationship to a wide range of physiological processes, as well as the onset and progression of several diseases. As a result, studies and applications involving exosomes rely heavily on their collection and analysis [14, 28-30]. However, there are many drawbacks to the conventional ways of isolating exosomes, such as the time and effort required and the high cost of the necessary equipment and chemicals. Microfluidic technology has the benefits of great sensitivity and efficiency when it comes to exosome separation, in comparison to conventional approaches. Microfluidic technology has recently facilitated effective separation, enrichment, and detection of different exosome information on a single chip, thanks to increased research and technological advancements. This suggests that point-of-care

© 2024, LLC Science and Innovations, Saratov, Russia

testing and other therapeutic applications of microfluidic chips have a lot of promise [6, 13, 14, 17, 28-30].

This study is comparable to others that have used anti-CD9 immuno-affinity magnetic beads conjugated with streptavidin and biotin to separate plasma samples with good sensitivity and efficiency. Furthermore, there is no restriction on the sample size when using bead-based procedures. A different study found that immunoaffinity isolation using anti-CD9 conjugated, anti-CD81, and antibody cocktail-linked magnetic nanowires magnetic beads could achieve a yield that was almost three times higher than that of classical approaches. In comparison to results obtained using more traditional approaches, Tim4, which binds exclusively to the phosphatidylserine on the surface of exosome cells, shown much less contamination [31-33].

The introduction of microfluidic devices has improved isolation and detection procedures by making it easier to screen for, separate, and capture exosomes immunologically. For this reason, they are highly desirable subjects for research into disease detection. The cargo of exosomes, which consists of certain proteins and nucleic acids, has been the subject of multiple investigations as a potential biomarker source in biofluids [34-37]. In addition to traditional DNA analysis, RNA analysis of exosomes in liquid biopsy samples may shed light on some processes and, in the long run, open the door to individualized therapy. In light of these considerations, microfluidic liquid biopsy may also prove to be a significant tactic in the quest for disease monitoring and individualized targeted treatment [38]. Addressing the obstacles to clinical translation and clinical application of exosomes as biomarker sources will primarily be the focus of research into microfluidic devices [39]. New microfluidic LOC platforms are always under development with the goals of making isolation more sensitive and making in situ analysis even easier. The present trend and desire for the development of "smart" systems that are both highly functional and easy to use, especially for those without a background in POCT, are congruent with this [23]. Furthermore, the initial stride towards individualized healthcare may lie in the development, standardization, and utilization of such cutting-edge technology. It might also help get us closer to the faraway aim of building a machine that can separate and analyses all components of a liquid biopsy in one go, which would pave the way for more accurate predictive medicine and more individualized treatment plans [23]. Overcoming the complexity and difficulties of clinical trials and validation is also necessary for such technology to gain widespread acceptance among medical practitioners worldwide. In addition, perfecting technology, increasing platform dynamic range, and producing sensitive, particular, and cost-effective devices for personalized medicine is the ultimate challenge in the clinic [4, 8, 17].

One specific method for separating exosomes that can be used with microfluidic devices is immunoaffinity-based particle entrapment. Using antibody-conjugated magnetic beads to separate exosomes has been the subject of multiple investigations. We evaluated CD9-conjugated magnetic beads of varying sizes for plasma exosome separation using an external force to move the beads; the results showed efficiencies that were 10-15 times greater than those of ultracentrifuges [27]. Better circumstances for the interaction between vesicles and ligands on the beads were created when antibodies conjugated magnetic beads were incubated with solutions containing exosomes, according to their findings. There is no upper limit on the number of samples that can be used using bead-based methods. Additionally, pancreatic cancer patients' plasma exosomes were processed using the immunoaffinity chromatography (CD63) microfluidic technology. In order to directly extract RNA and protein from the exosomes, the separation depends on receptors that receive extra input to add lysis buffer. One alternative method for microfluidic device design involved labelling exosomes on the chip with fluorescent dye through an input channel. This allowed for the exosomes to be quantified on the chip. Exosomes were quickly and easily quantified using a fluorescence assay and a microfluidic system that separated them on a chip. In order to separate exosomes from ovarian cancer, researchers looked into alternative microfluids that used photo-lithography techniques based on micro-dimensional sites of graphene oxide (GO)/polydopamine (PDA) covered with protein G. There is hope that the proposed method can employ exosomes for diagnostic and prognostic purposes [27].

Medications used to treat cancer can shrink tumors or even put patients into a temporary remission. But as time went on, cancer cells developed resistance to chemotherapy. A cure for cancer patients is still elusive due to drug resistance. Exosomes produced by MSCs have therapeutic potential for cancer treatment and for increasing cancer cells' sensitivity to chemotherapy. The miR-302a found in hucMSC exosomes inhibited the proliferation and metastasis of cancer cells, as an example. Other research found that hucMSC-derived exosomes made K562 cells more sensitive to IM. It appears that miR-146a-5p has an additional role in the development of IM resistance, as it is downregulated in CML patients, particularly those with the disease. Myeloid neoplasm chronic myeloid leukemia (CML) is caused by the BCR-ABL fusion gene, which interferes with downstream signaling pathways to induce dysregulated cellular proliferation and resistance to apoptosis. New evidence suggests an inverse relationship between miR-150 levels and BCR-ABL transcript levels, with miR-150 levels being substantially elevated after BCR-ABL tyrosine kinase activity is reduced. Additionally, miR-155, miR-564, and miR-31 all showed decreased expression levels in CML, and BCR-ABL activity played a role in this [7, 40-42].

Conclusion

In conclusion, we pioneered a straightforward microfluidic method based on immunoaffinity to separate exosomes according to their drug loading capacity. With a little volume needed and a high-speed extraction technique, the developed system was able to separate exosome with excellent sensitivity, recovery rate, and purity. For therapeutic applications, the chip could be scaled up to allow high-throughput extraction of exosomes that can load drugs. Because of this, this platform should prove to be an invaluable resource for future personal diagnostic gadgets and clinical applications of personalized medicine.

Acknowledgements

This study was carried out in the form of a project approved under the number 99314850605 of the Faculty of Modern Medical Technologies of Tehran University of Medical Sciences.

Funding

This study was supported by the Tehran University of Medical Sciences [grant no. 99-3-148-50605].

© 2024, LLC Science and Innovations, Saratov, Russia

Availability of data and materials

The datasets used and/or analyzed during the current study are available from the corresponding author on reasonable request.

Author contributions

Amir Monfaredan analyzed data. Amir Monfaredan wrote the manuscript. Amir Monfaredan and Elahe Motevaseli contributed to the study concept, and drafted and revised the manuscript. Amir Monfaredan and Elahe Motevaseli confirm the authenticity of all the raw data. All authors read and approved the final version of the manuscript.

Ethics approval and consent to participate

This study was approved by ethics code number IR.TUMS.MEDICINE.REC.1399.969 in the Ethics Committee of the Faculty of Medicine of Tehran University of Medical Sciences

Patient consent for publication

Not applicable

Conflict of interest

The authors declare no conflicts of interest.

References

1. Bernardi S, Farina M. Exosomes and extracellular vesicles in myeloid neoplasia: The multiple and complex roles played by these "*Magic bullets*". *Biology (Basel)* 2021; 10(2): 105. https://doi.org/10.3390/biology10020105.
2. Bernardi S, Foroni C, Zanaglio C, Re F, Polverelli N, Turra A, et al. Feasibility of tumor-derived exosome enrichment in the onco-hematology leukemic model of chronic myeloid leukemia. *Int J Mol Med* 2019; 44(6): 2133-2144. https://doi.org/10.3892/ijmm.2019.4372.
3. Gamage SST, Pahattuge TN, Wijerathne H, Childers K, Vaidyanathan S, Athapattu US, et al. Microfluidic affinity selection of active SARS-CoV-2 virus particles. *Sci Adv* 2022; 8(39): eabn9665. https://doi.org/10.1126/sciadv.abn9665.
4. Li Y, Cai T, Liu H, Liu J, Chen SY, Fan H. Exosome-shuttled miR-126 mediates ethanol-induced disruption of neural crest cell-placode cell interaction by targeting SDF1. *Toxicol Sci* 2023; 195(2): 184-201. https://doi.org/10.1093/toxsci/kfad068.
5. Jafarzadeh N, Gholampour MA, Alivand MR, Kavousi S, Arzi L, Rad F, et al. CML derived exosomes promote tumor favorable functional performance in T cells. *BMC Cancer* 2021; 21(1): 1002. https://doi.org/10.1186/s12885-021-08734-3.
6. Kang KW, Jung JH, Hur W, Park J, Shin H, Choi B, et al. The potential of exosomes derived from chronic myelogenous leukaemia cells as a biomarker. *Anticancer Res* 2018; 38(7): 3935-3942. https://doi.org/10.21873/anticanres.12679.
7. Keramati F, Jafarian A, Soltani A, Javandoost E, Mollaei M, Fallah P. Circulating miRNAs can serve as potential diagnostic biomarkers in chronic myelogenous leukemia patients. *Leuk Res Rep* 2021; 16: 100257. https://doi.org/10.1016/j.lrr.2021.100257.
8. Lan X, Yu R, Xu J, Jiang X. Exosomes from chondrocytes overexpressing miR-214-3p facilitate M2 macrophage polarization and angiogenesis to relieve Legg Calve-Perthes disease. *Cytokine* 2023; 168: 156233. https://doi.org/10.1016/j.cyto.2023.156233.
9. Li MY, Zhao C, Chen L, Yao FY, Zhong FM, Chen Y, et al. Quantitative proteomic analysis of plasma exosomes to identify the candidate biomarker of imatinib resistance in chronic myeloid leukemia patients. *Front Oncol* 2021; 11: 779567. https://doi.org/10.3389/fonc.2021.779567.
10. Li P, Chen J, Chen Y, Song S, Huang X, Yang Y, et al. Construction of exosome SORL1 detection platform based on 3D porous microfluidic chip and its application in early diagnosis of colorectal cancer. *Small* 2023; 19(20): e2207381. https://doi.org/10.1002/smll.202207381.
11. Li Y, Xu M, Zhu Z, Xu F, Chen B. Transendothelial electrical resistance measurement by a microfluidic device for functional study of endothelial barriers in inflammatory bowel disease. *Front Bioeng Biotechnol* 2023; 11: 1236610. https://doi.org/10.3389/fbioe.2023.1236610.
12. Lu RXZ, Rafatian N, Zhao Y, Wagner KT, Beroncal EL, Li B, et al. Heart-on-a-chip model of immune-induced cardiac dysfunction reveals the role of free mitochondrial DNA and therapeutic effects of endothelial exosomes. *bioRxiv* [Preprint]. 2023: 2023.08.09.552495. https://doi.org/10.1101/2023.08.09.552495.
13. Pattabiraman PP, Feinstein V, Beit-Yannai E. Profiling the miRNA from exosomes of non-pigmented ciliary epithelium-derived identifies key gene targets relevant to primary open-angle glaucoma. *Antioxidants (Basel)* 2023; 12(2): 405. https://doi.org/10.3390/antiox12020405.
14. Han Z, Peng X, Yang Y, Yi J, Zhao D, Bao Q, et al. Integrated microfluidic-SERS for exosome biomarker profiling and osteosarcoma diagnosis. *Biosens Bioelectron* 2022; 217: 114709. https://doi.org/10.1016/j.bios.2022.114709.
15. Hu M, Brown V, Jackson JM, Wijerathne H, Pathak H, Koestler DC, et al. Assessing breast cancer molecular subtypes using extracellular vesicles' mRNA. *Anal Chem* 2023; 95(19): 7665-7675. https://doi.org/10.1021/acs.analchem.3c00624.
16. Jafarzadeh N, Safari Z, Pornour M, Amirizadeh N, Forouzandeh Moghadam M, Sadeghizadeh M. Alteration of cellular and immune-related properties of bone marrow mesenchymal stem cells and macrophages by K562 chronic myeloid leukemia cell derived exosomes. *J Cell Physiol* 2019; 234(4): 3697-3710. https://doi.org/10.1002/jcp.27142.
17. Lin S, Zhu B. Exosome-transmitted FOSL1 from cancer-associated fibroblasts drives colorectal cancer stemness and chemo-resistance through transcriptionally activating ITGB4. *Mol Cell Biochem* 2023. https://doi.org/10.1007/s11010-023-04737-9.
18. Mineo M, Garfield SH, Taverna S, Flugy A, De Leo G, Alessandro R, et al. Exosomes released by K562 chronic myeloid leukemia cells promote angiogenesis in a Src-dependent fashion. *Angiogenesis* 2012; 15(1): 33-45. https://doi.org/10.1007/s10456-011-9241-1.
19. Wan Z, Chen X, Gao X, Dong Y, Zhao Y, Wei M, et al. Chronic myeloid leukemia-derived exosomes attenuate adipogenesis of adipose derived mesenchymal stem cells via transporting miR-92a-3p. *J Cell Physiol* 2019; 234(11): 21274-21283. https://doi.org/10.1002/jcp.28732.
20. Ninfa AJ, Ballou DP, Benore M. Fundamental laboratory Approaches for Biochemistry and Biotechnology. John Wiley & Sons; 2009; 480 p. https://www.wiley.com/en-us/Fundamental+Laboratory+Approaches+for+Biochemistry+and+Biotechnology,+2nd+Edition-p-9780470471319.
21. Patterson SD, Copland M. The Bone Marrow Immune Microenvironment in CML: Treatment responses, treatment-free remission, and therapeutic vulnerabilities. *Curr Hematol Malig Rep* 2023; 18(2): 19-32. https://doi.org/10.1007/s11899-023-00688-6.
22. Song F, Wang C, Wang C, Wang J, Wu Y, Wang Y, et al. Multi-phenotypic exosome secretion profiling microfluidic platform for exploring single-cell heterogeneity. *Small Methods* 2022; 6(9): e2200717. https://doi.org/10.1002/smtd.202200717.
23. Surappa S, Multani P, Parlatan U, Sinawang PD, Kaifi J, Akin D, et al. Integrated "lab-on-a-chip" microfluidic systems for isolation, enrichment, and analysis of cancer biomarkers. *Lab Chip* 2023; 23(13): 2942-2958. https://doi.org/10.1039/d2lc01076c.
24. Taverna S, Amodeo V, Saieva L, Russo A, Giallombardo M, De Leo G, et al. Exosomal shuttling of miR-126 in endothelial cells modulates adhesive and migratory abilities of chronic myelogenous leukemia cells. *Mol Cancer* 2014; 13: 169. https://doi.org/10.1186/1476-4598-13-169.

© 2024, LLC Science and Innovations, Saratov, Russia

25. Wang QS, Xiao RJ, Peng J, Yu ZT, Fu JQ, Xia Y. Bone marrow mesenchymal stem cell-derived exosomal KLF4 alleviated ischemic stroke through inhibiting N6-methyladenosine modification level of Drp1 by targeting lncRNA-ZFAS1. *Mol Neurobiol* 2023; 60(7): 3945-39462. https://doi.org/10.1007/s12035-023-03301-2.
26. Corrado C, Raimondo S, Saieva L, Flugy AM, De Leo G, Alessandro R. Exosome-mediated crosstalk between chronic myelogenous leukemia cells and human bone marrow stromal cells triggers an interleukin 8-dependent survival of leukemia cells. *Cancer Lett* 2014; 348(1-2): 71-76. https://doi.org/10.1016/j.canlet.2014.03.009.
27. Fonseca-Benitez A, Romero-Sanchez C, Lara SJP. A rapid and simple method for purification of nucleic acids on porous membranes: Simulation vs. experiment. *Micromachines (Basel)* 2022; 13(12): 2238. https://doi.org/10.3390/mi13122238.
28. Giallongo C, Parrinello NL, La Cava P, Camiolo G, Romano A, Scalia M, et al. Monocytic myeloid-derived suppressor cells as prognostic factor in chronic myeloid leukaemia patients treated with dasatinib. *J Cell Mol Med* 2018; 22(2): 1070-1080. https://doi.org/10.1111/jcmm.13326.
29. He L, Chen Y, Lin S, Shen R, Pan H, Zhou Y, et al. Regulation of Hsa-miR-4639-5p expression and its potential role in the pathogenesis of Parkinson's disease. *Aging Cell* 2023; 22(6): e13840. https://doi.org/10.1111/acel.13840.
30. Hrdinova T, Toman O, Dresler J, Klimentova J, Salovska B, Pajer P, et al. Exosomes released by imatinib-resistant K562 cells contain specific membrane markers, IFITM3, CD146 and CD36 and increase the survival of imatinib-sensitive cells in the presence of imatinib. *Int J Oncol* 2021; 58(2): 238-250. https://doi.org/10.3892/ijo.2020.5163.
31. Shi C, Pei S, Ding Y, Tao C, Zhu Y, Peng Y, et al. Exosomes with overexpressed miR 147a suppress angiogenesis and inflammatory injury in an experimental model of atopic dermatitis. *Sci Rep* 2023; 13(1): 8904. https://doi.org/10.1038/s41598-023-34418-y.
32. Wang M, Zhang Z, Li G, Jing A. Room-temperature self-healing conductive elastomers for modular assembly as a microfluidic electrochemical biosensing platform for the detection of colorectal cancer exosomes. *Micromachines (Basel)* 2023; 14(3): 617. https://doi.org/10.3390/mi14030617.
33. Wang M, Zhao H, Chen W, Bie C, Yang J, Cai W, et al. The SMAD2/miR-4256/HDAC5/p16^{INK4a} signaling axis contributes to gastric cancer progression. *Oncol Res* 2023; 31(4): 515-541. https://doi.org/10.32604/or.2023.029101.
34. Yu H, Wu Y, Zhang B, Xiong M, Yi Y, Zhang Q, et al. Exosomes derived from E2F1(-/-) adipose-derived stem cells promote skin wound healing via miR-130b-5p/TGFBR3 axis. *Int J Nanomedicine* 2023; 18: 6275-6292. https://doi.org/10.2147/ijn.s431725.
35. Yu Z, Tang H, Chen S, Xie Y, Shi L, Xia S, et al. Exosomal LOC85009 inhibits docetaxel resistance in lung adenocarcinoma through regulating ATG5-induced autophagy. *Drug Resist Updat* 2023; 67: 100915. https://doi.org/10.1016/j.drup.2022.100915.
36. Zhang X, Wang C, Huang C, Yang J, Wang J. Doxorubicin resistance in breast cancer xenografts and cell lines can be counterweighted by microRNA-140-3p, through PD-L1 suppression. *Histol Histopathol* 2023; 38(10): 1193-1204. https://doi.org/10.14670/hh-18-577.
37. Zhong AN, Yin Y, Tang BJ, Chen L, Shen HW, Tan ZP, et al. CircRNA Microarray Profiling Reveals hsa_circ_0058493 as a Novel Biomarker for Imatinib-Resistant CML. *Front Pharmacol* 2021; 12: 728916. https://doi.org/10.3389/fphar.2021.728916.
38. Wang Y, Wang S, Chen A, Wang R, Li L, Fang X. Efficient exosome subpopulation isolation and proteomic profiling using a Sub-ExoProfile chip towards cancer diagnosis and treatment. *Analyst* 2022; 147(19): 4237-4248. https://doi.org/10.1039/d2an01268e.
39. Cetin Z, Ilker Saygili E, Yilmaz M. Crosstalk between CML cells with HUVECS and BMSCs through CML derived exosomes. *Front Biosci (Landmark Ed)* 2021; 26(3): 444-467. https://doi.org/10.2741/4901.
40. Chinnappan R, Ramadan Q, Zourob M. An integrated lab-on-a-chip platform for pre-concentration and detection of colorectal cancer exosomes using anti-CD63 aptamer as a recognition element. *Biosens Bioelectron* 2023; 220: 114856. https://doi.org/10.1016/j.bios.2022.114856.
41. Edlinger L, Berger-Becvar A, Menzl I, Hoermann G, Greiner G, Grundschober E, et al. Expansion of BCR/ABL1$^+$ cells requires PAK2 but not PAK1. *Br J Haematol* 2017; 179(2): 229-241. https://doi.org/10.1111/bjh.14833.

Authors:
Amir Monfaredan – PhD, Associated Professor, Department of Molecular Medicine, School of Advanced Technologies in Medicine, Tehran University of Medical Sciences, Tehran, Iran. https://orcid.org/0009-0008-2016-0198.
Fakher Rahim – PhD, College of health sciences, Cihan university-Sulaymaniya, Kurdistan region, Iraq. https://orcid.org/0000-0002-2857-4562.
Gholamreza Tavoosidana – PhD, Associated Professor, Department of Molecular Medicine, School of Advanced Technologies in Medicine, Tehran University of Medical Sciences, Tehran, Iran. https://orcid.org/0000-0002-1079-7434.
Mohammad Hossein Modarressi – PhD, Associated Professor, Department of Medical Genetics, Faculty of Medicine, Tehran University of Medical Sciences, Tehran, Iran. https://orcid.org/0000-0003-2763-1964.
Alaviyehsadat Hosseininasab – PhD, GeneDia Life science company, Tehran, Iran. https://orcid.org/0000-0003-2290-1005.
Ali-Akbar Aghajani-Afrouzi – Associated Professor, Department of Business Administration, Payame Noor University, Tehran, Iran. https://orcid.org/0000-0002-4198-8655.
Mahdi Shafiee Sabet – Associated Professor, Neurologist, School of Medicine, Tehran University of Medical Sciences, Tehran, Iran. https://orcid.org/0009-0006-8954-8428.
Elahe Motevaseli – PhD, Associated Professor, Department of Molecular Medicine, School of Advanced Technologies in Medicine, Tehran University of Medical Sciences, Tehran, Iran. https://orcid.org/0000-0002-9723-2590.

© 2024, LLC Science and Innovations, Saratov, Russia

Supplementary

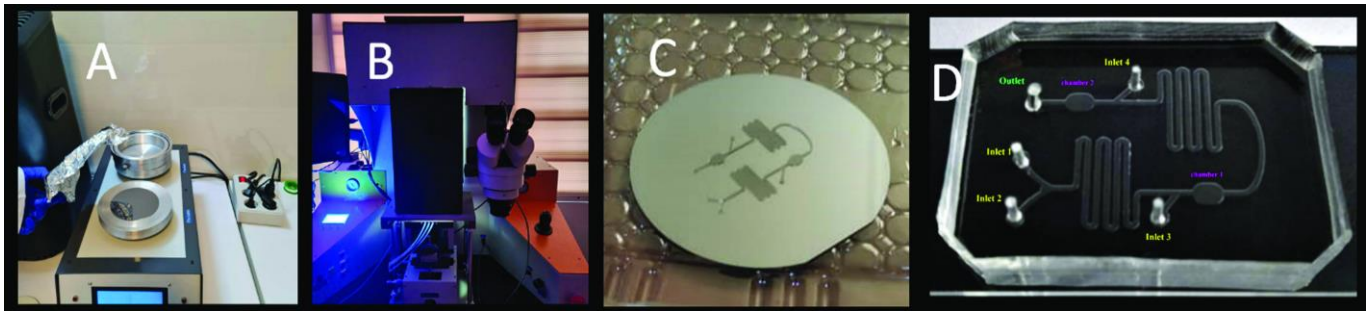

Figure S1. A: the steps of baking the wafer at temperatures of 60 and 95 degrees Celsius, B: the exposure process on the lined mask on the wafer, C: the final mold after the impact of the developer and washing with isopropanol, and D the final mold of the PDMS chip.

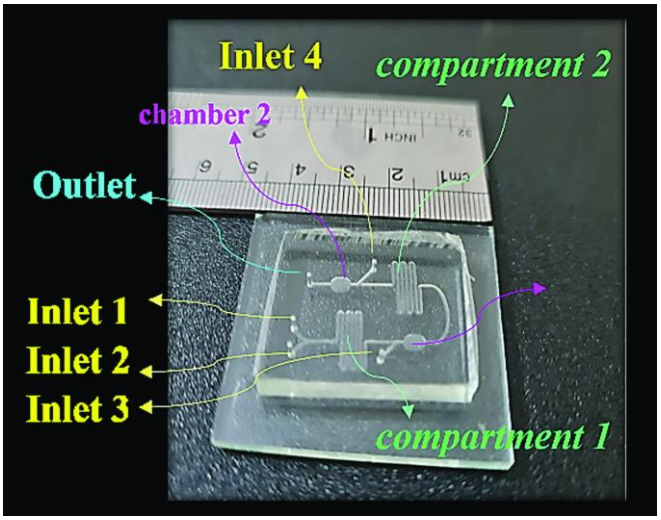

Figure S2. The variety of inputs, chambers, channels and output of the chip. In summary, entrance 1 and 2 are the place of injection of suspension containing exosome and specific magnet, entrance 3 is the entrance of PBS, chamber 1, the place where mixing is stopped by that trap, and entrance 4 is the place of imatinib loading.

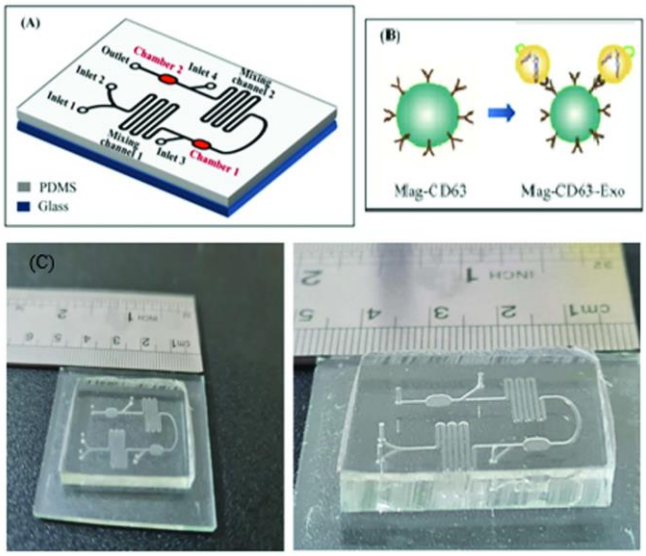

Figure S3. The schematic illustration of (A) and (C) microfluidic chip and (B) the principles of immunoaffinity-based exosome separation.

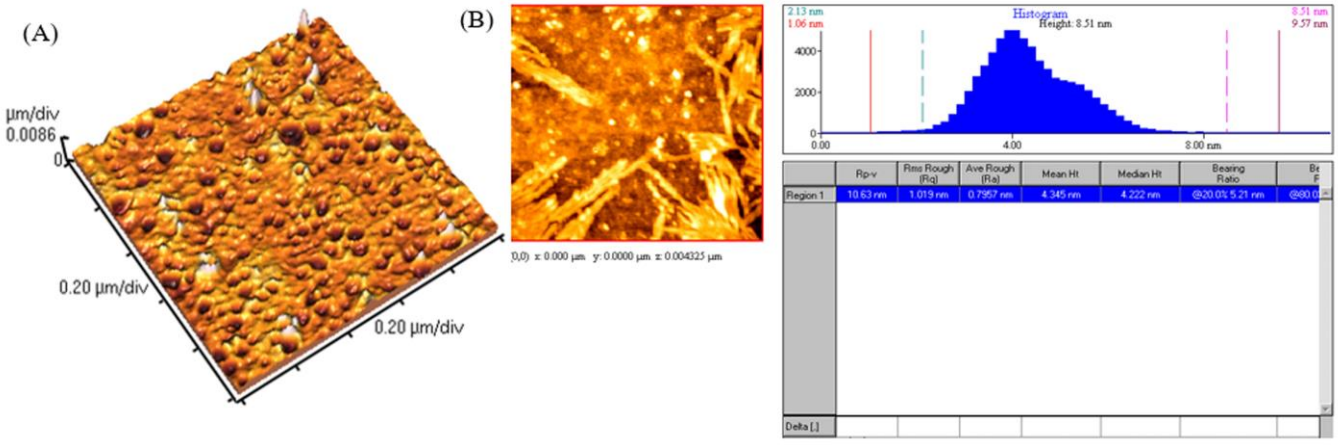

Figure S4. (A) 3D and (B) 2D images of the SU-8 100 chip surface.